FLOW PATTERN IN A CONVERGE 90° DEGREE BEND

M. Taghizadeh[1], T. Hosseyni Serghin[2], M. Bazargan[3], & S. Nazari[4]

[1]Department of Civil Engineering, Tabriz University, Tabriz, Iran
[2]Department of Civil Engineering, Islamic Azad University, Central Tehran Branch, Tehran, Iran
[3]Department of Civil Engineering, Islamic Azad University, Tehran West Branch, Tehran, Iran
[4]Department of Civil Engineering, Islamic Azad University, Eglid Branch, Fars, Iran
E-mail: taghizadeh.mortaza@gmail.com

Abstract

Flow pattern in a bend is one of the most complex water flows in nature. In real life the width of meander is not constant always. This paper describe flow pattern in a converge 90° degree bend experimentally and numerically where the width of channel varies from 0.6m to 0.3m along the bend. The PVM velocimeter was used to measure the longitudinal and lateral components of velocity. The numerical model, SSIIM, used in this study, solves Reynolds-averaged Navier-stokes equations and continuity equation to calculate flow field. By comparison of the numerical result with experimental data, SSIIM was found to simulate flow pattern in converge 90° degree bend with sufficient accuracy.

Introduction

In channel bend imbalance between the transverse water surface gradient force and centrifugal force generates secondary current. Therefore flow characteristics in channel bends will be much more complicated than those in straight reach. Flow patterns in sharp and mild bends are different from each other. In sharp bend maximum velocity takes place near the inner wall along bend while at the mild bend maximum velocity at the start of bend takes place near the inner wall and at the end of it transfer to outer wall due to secondary flow. Many researchers have been carried out on curved channels. Leschziner and Rodi (1979), Ye and McCorquodale (1998) simulated flow patter in curved open channel. Georgia and Smith (1986) represent that in a curved converging channel result of computational model agree with experimental results. Naji Abhari et al. (2010) investigate flow pattern and strength of secondary flow in 90 degree bend. Rezofski (1957) studied flow pattern bed elevation in 90 degree bend. Bahrami Jovein et al. (2009) showed that transverse slope of water surface in a bend is not linear. Odgaared (1989) find out the velocity and depth of flow in the axis of curve in the channel was constant. Wilson et al. (2003) computed the fully developed three dimensional velocity distributions in a meandering channel. Blanckart and Graf (2001), Blanckart (2002); Booij (2002) measured flow velocity in meandering channel experimentally. Review of researches show that flow pattern in converge curved channel is still not well studied. In order to better understanding of flow pattern in converge curved channel we have to investigate the flow filed characteristics such as: velocity profile, secondary flow, distribution of turbulent kinetic energy, distribution of turbulent dissipation and bed shear stress. This study focuses on the mentioned characteristics which are not observed well at previous studies.

Laboratory Set Up

Experiments were conducted utilizing the facilities available at the hydraulic engineering laboratory of Islamic Azad University, science and research branch. Laboratory channel, made of Plexiglas (Manning roughness coefficient is 0.008), consist of three parts. The first part is straight channel with 4.5m length and 60cm wide. This part followed by 90° bend with a constant radius of curvature of R=1.7m on the centerline. Wide of bend varies from 60cm to 30cm along it. At the downstream of bend there is another straight channel with 2m length and 30cm wide. At the end of channel there is a reservoir.

Figure 1: Schematic view of converge 90° channel

Measurement of discharge was done by trapezoid wire. Depth of flow was measured by a digital point gage. The flow velocity was measured by a digital velocimeter PVM. The components of velocity were measured at 5 different levels of water depth and at 7 different lateral distances along the width of channel. The measured sections were selected radially at every 10°. Experiments were conducted for discharge of 18.45 $\frac{L}{S}$. Figure 1 shows view of converge 90° channel.

Numerical Model

Numerical model used in this study was SSIIM. SSIIM was developed by Olsen (2002). The discretization method was base on a finite volume approach (Olsen 2002). The flow field was computed by solving the Reynolds-averaged Navier-Stokes equations and continuity equation using the $(k-\varepsilon)$ turbulence model (Rodi 1980).

$$\frac{\partial \mathrm{U_i}}{\partial \mathrm{x_i}} \tag{1}$$

$$\frac{\partial \mathrm{U_i}}{\partial \mathrm{t}} + U_j \frac{\partial \mathrm{U_i}}{\partial \mathrm{x_j}} = \frac{1}{\rho}\frac{\partial}{\partial \mathrm{x_i}}\left(-P\delta_{ij} - \rho\overline{u_\iota u_j}\right) \tag{2}$$

where, $\mathrm{U_i}(\mathrm{i}=1,2,3)$ are the velocity component, (x) is the spatial geometrical scale, ρ is the water density, (P) is the pressure, δ is the Kronecker delta and (u) is the velocity fluctuation over time during time step Δt. The SSIIM model computes the turbulent stresses $\left(\overline{u_\iota u_j}\right)$, using the eddy viscosity relation:

$$-\overline{u_\iota u_j} = \nu_\mathrm{t}\left(\frac{\partial \mathrm{U_i}}{\partial \mathrm{x_j}} + \frac{\partial \mathrm{U_j}}{\partial \mathrm{x_i}}\right) - \frac{2}{3}k\delta_{ij} \tag{3}$$

In which:

$$\nu_\mathrm{t} = \frac{c_\mu . k^2}{\varepsilon} \tag{4}$$

Where, ν_t is eddy viscosity, c_μ is a coefficient, k is turbulent kinetic energy and ε is its dissipation rate. The SIMPLE method (Patankar, 1980) was used to compute the pressure. Boundary conditions are used in this model consist of: Dirichlet boundary conditions at the inflow boundary, zero gradient boundary conditions at out flow boundaries for all variables and wall law at bed and walls. At water surface zero gradient boundary conditions are used for ε and turbulent kinetic energy, k, is set to zero. SSIIM offers different numerical methods for calculation of the free surface including: a rigid lid approach where a standard backwater method is initially used, and a method by which the free surface is updated from the computed pressure field.

Velocity Profiles

Figure 2 shows velocity profiles at 30°, 60° and 90° sections. The velocity profiles are resultant lateral and vertical component of velocity. This figure indicates that at 30° section where the strength of secondary flow is not enough the velocity profiles are almost logarithmic. At the end of bend the maximum velocity does not take place at the water surface due to secondary flow. This subject is more obvious at inside bend. Comparison of numerical simulation and experimental data shows that SSIIM is capable to simulate velocity profiles at 90° converge bend. In this figure Z is depth and Y is distance from inside bend.

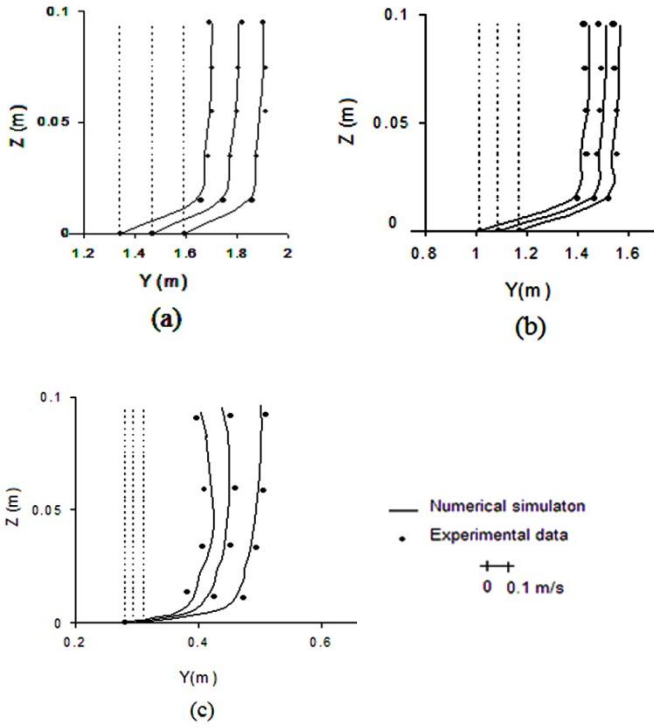

Figure 2: Distribution of velocity at sections, a) 30°, b) 60° and c) 90°

Velocity Vectors

Formation of secondary flow has important influence on velocity vectors. Figure (3a) shows that at 30° section there is a unilateral flow toward inside bend because at this zone the strength of pressure gradient is higher than the strength of centrifugal force. When the strength of secondary flow grows up along the bend, in some ports of cross sections the velocity vectors at higher water level (away from bed) tend to outside bend. This phenomenon is more obvious at 90° cross section than 60° cross section. The direction of velocity vectors at these cross sections near the bed are

toward to inside bend due to pressure gradient. Furthermore these figures indicate that since width of channel varies along the bend, obvious circulation zone due to secondary flow does not form at cross sections.

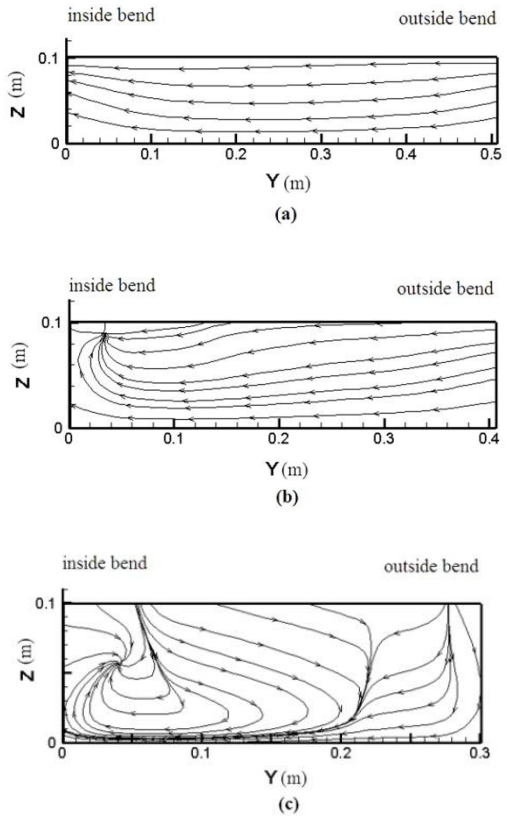

Figure 3: Velocity vectors at different vertical sections a) 30°, b) 60° and c) 90°

Contours of Longitudinal Velocity

In this section we investigate influence of secondary flow on contours of longitudinal velocity at different cross sections along the bend. Fig (4a) shows contours of longitudinal velocity at 30° section. In this section there is a maximum velocity zone near the inside bend because at this section the strength of secondary flow is not enough for transferring lateral momentum to outside bend. When the secondary flow grows along the bend (i.e. 60° and 90° sections) the maximum velocity zone extend to outside bend. This subject at 90° section is more obvious than 60° section.

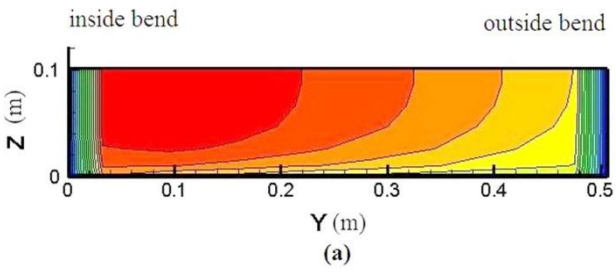

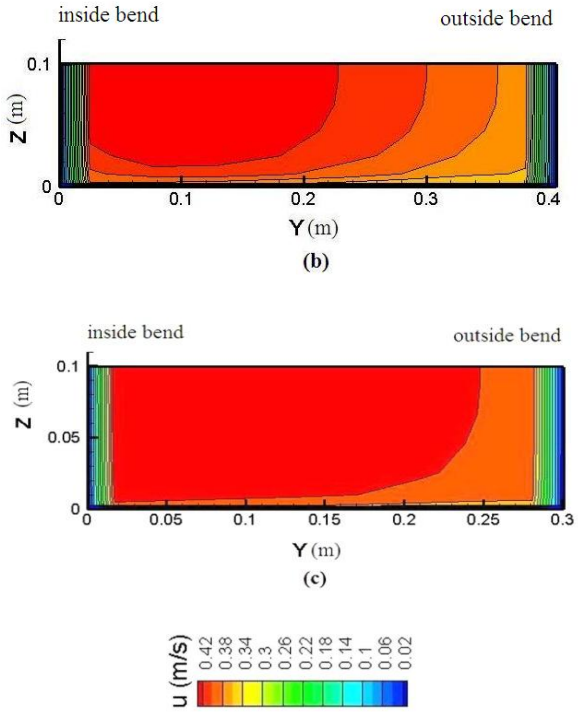

Figure 4: Contours of longitudinal velocity at different vertical sections a) 30°, b) 60° and c) 90°

Distribution of Turbulent Kinetic Energy

At straight channel the maximum of turbulent kinetic energy takes place near the bed. Roughness produces turbulent at the bed, but when water level increases turbulent kinetic energy decrease. Therefore minimum turbulent kinetic energy takes place at water surface. Distribution of turbulent kinetic energy at channel bend is like straight channel. But at the channel bend there is another zone near the inside bend that its turbulent kinetic energy is high (i.e. 60° section). For confluence of velocity vectors due to formation of secondary flow, Fig (3b) we expect a zone with high turbulent kinetic energy near the inside bend. At the end of bend Fig (5c) when the secondary flow extends completely another zone with high turbulent kinetic energy forms near the outside bend.

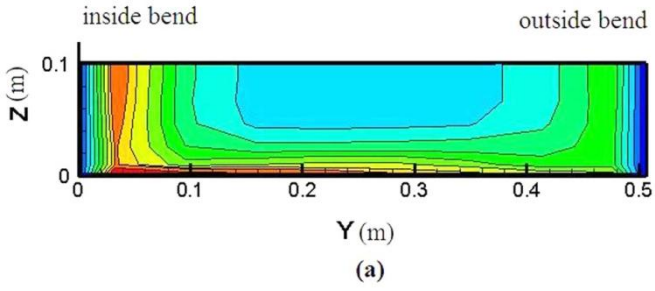

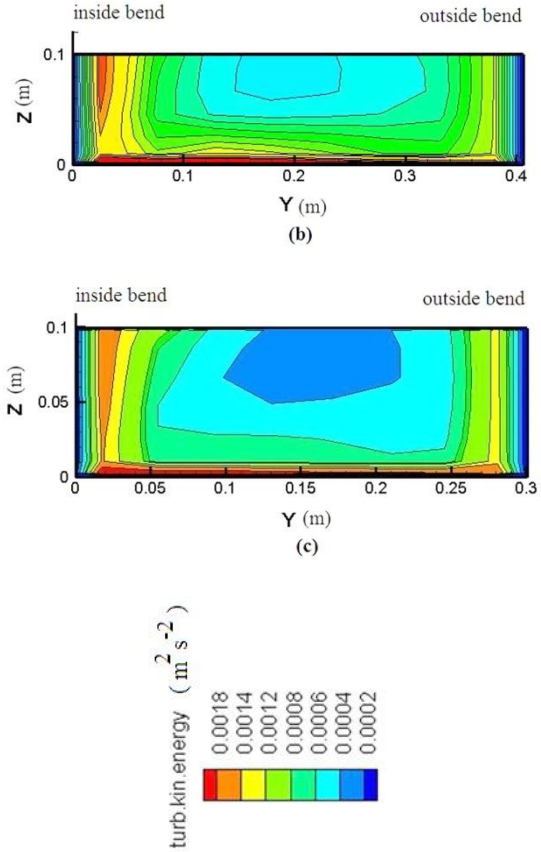

Figure 5: Distribution of turbulent kinetic energy at different vertical sections a) 30°, b) 60° and c) 90°

Distribution of Turbulent Dissipation

Figure (6) shows distribution of turbulent dissipation at different vertical section along the bend. This figure indicates that the maximum of turbulent dissipation takes place near the bed. This subject displays that bed roughness is main mechanism for turbulent dissipation too. According to this figure, the turbulent dissipation zone at the end of bend (Fig 6c) is bigger than the turbulent dissipation zone at the start of bend (Fig 6a). Furthermore this figure shows that minimum turbulent dissipation zone takes place at the water surface.

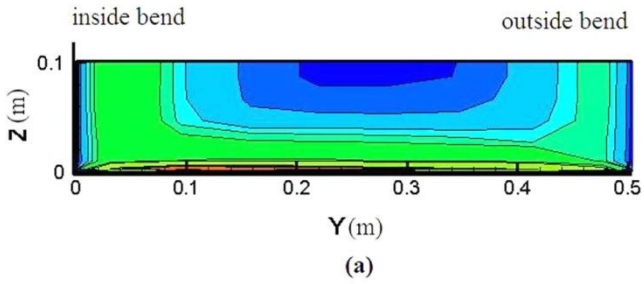

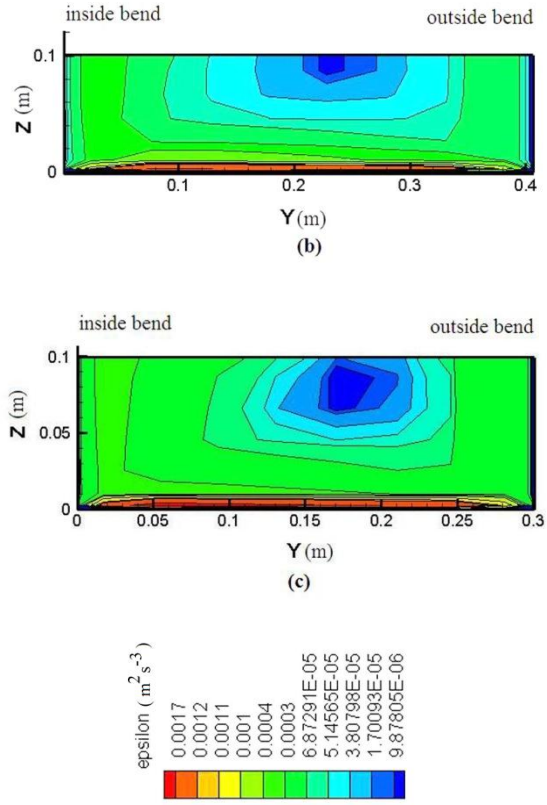

Figure 6: Distribution of turbulent dissipation at different vertical sections a) 30°, b) 60° and c) 90°

Bed Shear Stress

In channel bend the distribution of shear stress is not symmetrical to the central axis of the channel. It changes along length of bend due to secondary flow. Figure 7 shows bed shear stress along the channel. This figure indicates that the maximum of bed shear stress takes place near the end of bend. Since correlation between shear stress and flow velocity is high we expect that maximum shear stress takes place at the end of bend (Fig 4-c confirms this subject).

Figure 7: bed shear stress along the channel

Conclusion

This analysis permits the following important conclusion:

- At the end of converge 90° degree bend the maximum velocity does not take place at the water surface.
- The direction of velocity vectors at different cross sections near the bed are toward to inside bend due to pressure gradient.
- When the secondary flow grows along the bend (i.e. 60° and 90° sections) the maximum velocity zone extends to outside bend.
- There is a zone with high turbulent kinetic energy near the inside bend. When the secondary flow extends completely at the end of bend, another zone with high turbulent kinetic energy forms near the outside bend.
- The turbulent dissipation zone at the end of bend is bigger than the turbulent dissipation zone at the start of bend and minimum turbulent dissipation zone takes place at the water surface.
- The maximum of bed shear stress takes place near the end of bend.
- Flow pattern in converge 90° degree bend can be simulated accurately by the numerical model, SSIIM.

References

Bahrami Jovein, E., Ghaneeizad, M., and Akhtari, A, A. (2009). Experimental Study on Flow Structure in Strongly Curved Open Channel 90-degree Bends. *International Symposium on Water Management and Hydraulic Engineering*,, (pp. 97-108). Macedonia, 1-5 September.

Blanckaert, K. (2002). Secondary currents measured in sharp open-channel bends. *International Conference on Fluvial Hydraulics*, (pp. 117-126). Louvain-la-Neuve, Belgium, 4-6 September: River Flow.

Blanckaert, K., and Graf, W.H. (2001). Mean flow and turbulence in open-channel bend. *J. Hydr. Engrg., ASCE, 127 (10)* , 835-847.

Booij, R. (2002). Modeling of the secondary flow structure in river bend. *International Conference on Fluvial Hydraulics* (pp. 127-134). Louvain-la-Neuve, Belgium, 4-6 September: Riwer Flow.

Georgia Dou,A,D., and Smith, K. (1986). Flow in curved converging channel. , *J. Hydr. Engrg., ASCE, 112(6),* , 476-496.

Leschziner, M. A. and Rodi, W. (1979). Calculation of Strongly Curved Open Channel Flow. *J. Hydr. Div., ASCE, 105(10)* , 1297-1314.

Naji Abhari, M., Ghodsian, M., Vaghefi, M.and Panahpur, N. (2010). Experimental and numerical simulation of flow in a 90° bend. *Flow Measurement and Instrumentation, 21* , 292-298.

Odgaard, A. (1989). River-meander model. *I: Development, J. Hydr. Engrg., ASCE,115(11)* , 1433-1450.

Olsen, N. R. (2002). *Hydroinformatics, fluvial hydraulics and limnology.* Norway: Dept. of hydraulic and Environmental Engineering, The Norwegian Univ. of Science and Technology.

Patankar, S. V. (1980). *Numerical heat transfer and fluid flow.* New York: McGraw-Hill Book.

Rodi, W. (1980). Turbulence models and their application in hydraulics. *Paseo Baja Virgen del Puerto 3, 28005* (pp. State-of-the-art paper). Madrid, Spain: IAHR.

Rozovskii, I. L. (1957). *Flow of water in bend of open channel.* Academy of sciences of the Ukrainian SSR , Institute of Hydraulic Engineering.

Wilson, C. A. M. E., Boxall, J. B., Guymer, I., and Olsen, N. R. B. (2003). Validation of a three dimensional numerical code in simulation of pseudo-natural meandering flows. *J. Hydr. Engrg., ASCE,129 (10)* , 785-768.

Ye, J., and McCorquodale, J. A. (1998). Simulation of curved open channel flows by 3D hydrodynamic model. *J. Hydr. Engrg., ASCE,124 (7)* , 687-698.